Light Backscattering Measurements of Small Particles in Microgravity

S-92.192 Special Assignment in Space Technology (3 cr)

Seppo Heikkilä, 49690F
Seppo dot Heikkila at iki dot fi

05.05.2004

Contents

1 Introduction

The objective of this study is to get experimental data on the lightscattering properties of dust particles in microgravity near the zero phase angle, i.e. when the angle between the light source and the observer seen from the observed object is near zero, in opposition. Opposition is important in astronomy because many light curve measurements can only be done near the zero phase angle. A good example of opposition is the full moon, where the lunar eclipse is observed at the zero phase angle. Small phase angles present a phenomenon called opposition effect, i.e. when the phase angle reaches about 10 degrees the light curve turns from linear to non-linear. Theoreticians have tried to explain this effect, and though many theories have been created, taking into account shadowing effects and multiple scattering, the phenomenon is not yet fully worked out. A serious restriction for creating a rigorous model of backscattering is that there are no experimental photometric measurements of a well defined dusty material near and at zero phase angle in microgravity.

Scattering measurements have and are being done in other phase angles in microgravity (e.g. $PROGRA^2$ Parabolic flight campaign [1], ICAPS proposal for the ISS), but they all have a serious restriction: they cannot measure very small phase angles. The problem is that in conventional experiments the detector gets in front of the light source in small phase angles, thus effectively blocking the light.

The big innovation in this experiment is the use of a beamsplitter, which first allows the incident light to pass and reflect to the sample, and then enables the scattered light from the sample to reach the detector. The aim is to get the first set of light scattering data near and at the zero phase angle for a well-established dusty lunar regolith analog material. The data is then compared with similar data measured in 1 g environment in order to gain better understanding of the effect that the packing density of dusty material has on its light scattering properties.

Our work involved designing a novel small phase angle goniometer, which flew with European Space Agency (ESA) Parabolic Flight Campaign number 36 between July 23rd. and August 1st. 2003. The experiment consists of five main parts; a CCD-camera with necessary optics, a diode laser, a beamsplitter attached to an adjustment tool, the sample container, and a laptop computer for controlling the CCD-camera.

1.1 Parabolic Flight Campaign

This study was part of 6.th European Space Agency (ESA)'s Student Parabolic Flight Campaign (SPFC), which took place between July 23rd. and August 1.st 2003 in Bordeaux, France. Our team, named as "Scattering@Zero-g“, had four members; astronomy students Jyri Näränen and Mikael Granvik from the Helsinki University, and Ville Saarinen and the author from the Helsinki University of Technology (HUT). Our experiment was sponsored by the Helsinki University of Technology (HUT), Automation Technology Laboratory from the HUT, Finnish Geodetic Institute (FGI) and The Department of Astronomy from the University of Helsinki. Most of the support came in the form of equipment, but eventually almost all of our expenses, e.g. our flights, were financed through sponsorship.

1.1.1 History

ESA has conducted Zero-G flights since 1984. Since October 1997 the Airbus A-300, based at the Bordeaux-Mérignac airport France, has been used by ESA and other space agencies for parabolic flights. The ESA Education Office started arranging SPFC in 1994 and the event has been annual since the year 2000. Students are selected through a design competition where students have to design an original experiment that can be carried out by two people in 20 seconds of microgravity. Four Finnish teams have attented SPFC between 1995-2004; in year 2000 one team from Tampere University of Technology and one from University of Oulu, in 2002 one team from HUT and finally our team in summer 2003 [2].

The primary goal of SPFC is to educate and motivate students to study science and technology. It is one of the most interesting ESA campaigns for the general public, and thus also a good PR-campaign. ESA has adopted the policy of flying a few journalists on each SPFC to report to the public on the on-going microgravity research sponsored by ESA. The French company Novespace is contracted by ESA to provide the campaign logistics and supervision of the experiment technical preparations [3]. The 'Centre d'Essais en Vol' (CEV, French Test Flight Centre) provides all the in-flight support and flying personnel. The aircraft technical support is given by the Bordeaux based Sogerma company.

1.1.2 Basics of parabolic flight

In parabolic flight, the aircraft is put into a sub-orbital trajectory that provides free-fall, i.e. weightlessness. This weightlessness experience, other than the duration, is exactly that experienced by astronauts on orbital missions. Each parabola begins by having the aircraft perform an aerobatic manoeuvre, which starts from the level flight and pitches up to approximately 45 degrees nose-high wings level, subjecting the passengers to a 2-g pull up lasting about twenty seconds. After that, the aircraft engines are powered back and the airplane is launched into the same parabolic trajectory that a ball would follow, providing everyone inside the airplane with around twenty seconds of weightlessness. At the bottom of the parabola, the aircraft slowly pulls out of its dive and levels off for the next arc, simultaneously restoring the weight to the cabin. All these procedures are shown in figure 1.

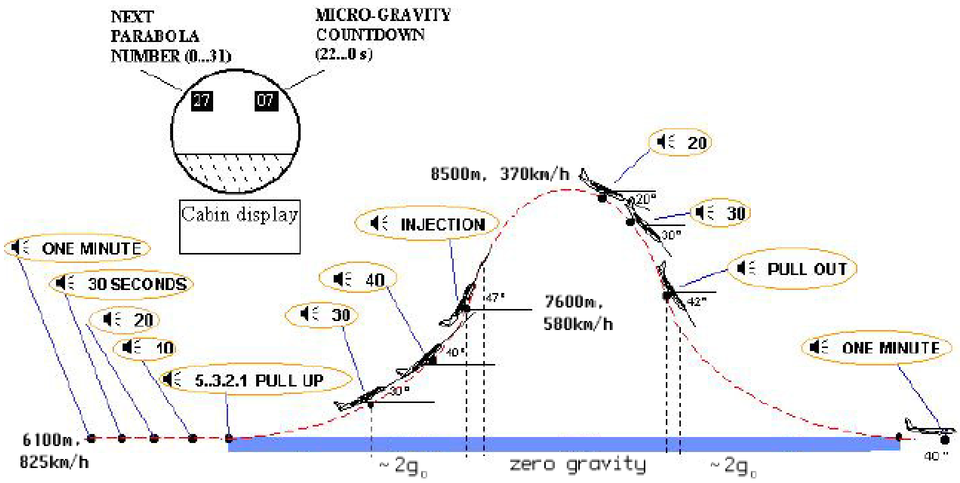

Figure 1: Flying procedures during one microgravity parabola.

A typical ESA campaign is scheduled for two weeks, with the first week dedicated to loading the experiment onto the aircraft and the second week devoted to the flights. The second week begins with a security briefing after which a familiarization flight of 5 parabolas is flown. The purpose of the familiarization flight is to familiarize the participants with the feeling of weightlessness, so that experimenters can act efficiently during the microgravity measurements. The actual experiment flights are carried out in two separate flights, each consisting of 31 parabolas.

The flying area is usually a military air space zone either over the Atlantic or Mediterranean Sea, depending on meteorological conditions and availability of air zones. In case of really bad weather or aircraft technical problems, a flight is delayed to the next day. Parabolic flights are considered as test flights, therefore particular precautions are taken to ensure that all in-flight operations are made safely. Prior to a campaign, support is provided to investigators in their equipment design and safety aspects. Most of the experiments are reviewed by experts during visits to investigators' home laboratories. A safety review is held one month before the campaign, where the integration of all equipment is discussed and the overall safety aspect of the campaign is assessed. Finally, a safety visit is made in the aircraft prior to the first flight to verify that all embarked equipment complies with safety rules [4].

All experimenters invited by ESA to participate on the parabolic flights must pass a medical examination required for a pilot's certificate with an additional tympanometry test, which tests how the tympanic membrane reacts to changes in air pressure. Due to the low and high gravity flight phases, motion sickness is quite common among participants of parabolic flights. Prior to the flights, anti-motion sickness medication is made available by request to flying participants.

2 Theory

When observing from Earth, outer solar system bodies are always seen at small phase angles due to the geometry of the situation, see figure 2. Phase angle is the angle between the light source and the observer seen from the observed object, as defined in figure 2. Significant part of the information in planetary astronomy is gained through light scattering, and thus the need for thorough empirical measurements is vital. Through these measurements semi-empirical models can be constructed, which typically include the effect of surface roughness and porosity. The two most-used semi-empirical systems are International Astronomical Union (IAU)'s HG system and Hapke's scattering law [6].

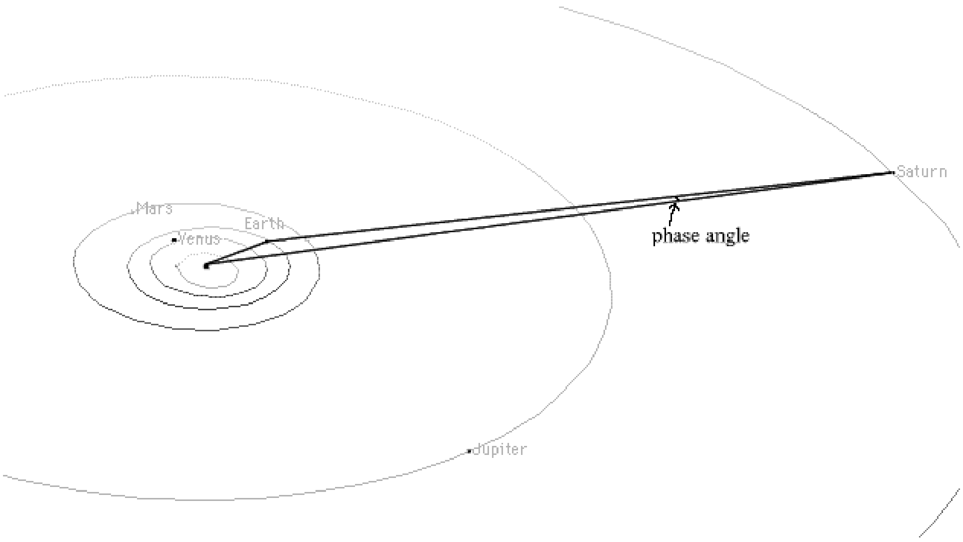

Figure 2: Phase angle between sun(light source), Earth(observer), and Saturn(observed object).

2.1 The opposition Effect

The opposition effect is a non-linear increase in the reflection brightness near and at zero phase angle. The intensity of the scattered light from the object is increasing linearly with decreasing phase angle due to the increases scattering area. However, when the phase angle reaches about 10 degrees, the light curve turns non-linear. The last few degrees before the zero phase angle present typically almost exponential increase in brightness, which is called the opposition spike. The effect is illustrated in figure 3.

The packing density also has a significant effect on the opposition effect. It is found that compression of the medium usually increases the brightness. For example a study made by Peltoniemi and Lumme showed that brightness with 10% packing density can be twice as bright as with 40% packing density for low albedo surfaces [5]. The effect of packing density is also studied in this experiment. These studies were mainly carried out by our team's principal investigator Jyri Näränen at the Department of Astronomy in Helsinki University [6].

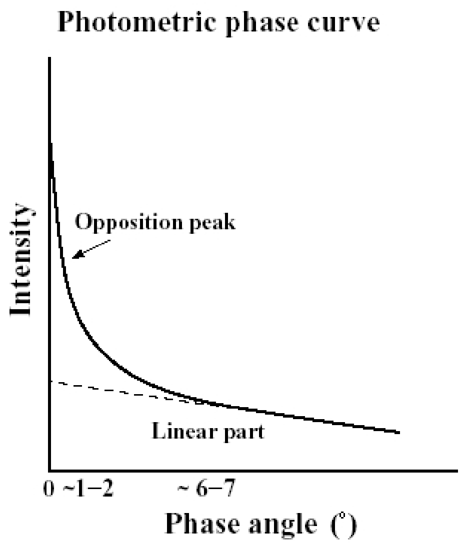

Figure 3: Opposition effect; increase in brightness turns non-linear near the zero phase angle.

A good example of the opposition effect is the full moon, which reaches zero phase-angle during an eclipse. Though the moon can never be seen from the Earth with phase-angles less than about 1°, the increase in brightness is about 40% between one day before full moon and during the full moon. The opposition effect can also be seen in a large variety of other materials, including terrestrial vegetation and satellites of outer planets. However, the effect is most distinct in powders with grain size less than 20μm, which is close to the grain size of the Apollo soil samples [7].

The basic light transfer models are inherently incapable of explaining the opposition effect. For small grain size powders, the intermolecular adhesive forces are comparable to the gravitational forces attracting them. Because of this, the microstructure of the powder can be porous and complex, and is often called a "fairy castle structure". This turns out to be just the kind of surface needed to explain the peculiar lunar photometric, polarization and thermal properties [7].

If particles are considerably larger than the light wavelength, the backscattering occurs by specular reflection from the first surface or through internal reflections from the inner surfaces. The fact that particles near the surface cast shadows on the deeper grains is thought to be one cause of the opposition effect. This is called shadow-hiding opposition effect, because the shadows are visible at large phase angles, but close to zero phase angle they are hidden by the objects that cast them [8].

If particles are approximately the same size as the wavelength, no distinct shadows can be defined, and thus no shadow-hiding can be observed. In this case another cause for opposition effect is suggested, called coherent backscattering. In this model waves traveling in multiply scattered paths within a non-uniform medium interfere constructively with each other constructing a peak at zero phase angle [9]. Several other phenomenon have been suggested to explain the opposition effect, such as spherical particles' glory and retroreflectance from randomly oriented crystals, but they are considered to be of minor importance for most medias [6].

The opposition effect can be examined in two different ways; as an absolute increase in brightness or as a relative increase to the extrapolated linear part of the phase curve. The difference between these definitions is that in the later form the opposition effect is considered as a separate phenomenon from the light backscattering. In the former, the opposition effect is considered as an inseparable part of the scattering phenomenon.

3 Experiment

The experiment setup used in our study is showed in figure 4. This experiment setup was designed and used in similar measurements in the FGI [10], and was further modified to suit the needs of the SPFC. The setup is simpler and more robust than what is traditionally used in scattering measurements. The zero phase angle is reached by first using a beamsplitter to reflect the light to the sample and then letting the scattered light from sample reach the CCD-camera. Other phase angles are achieved just by rotating the beamsplitter.

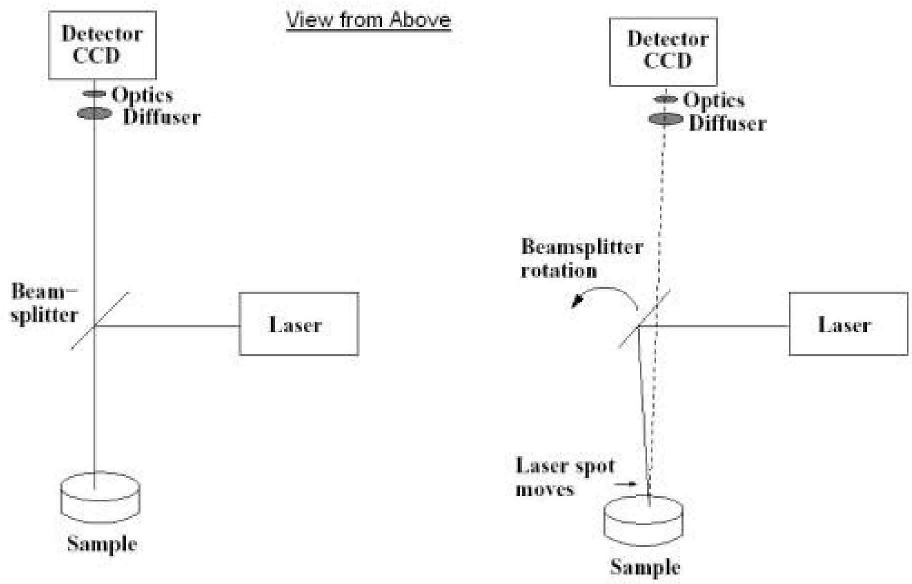

Figure 4: The experiment setup. The phase angle is changed by rotating the beamsplitter.

3.1 Building the experiment

We started building our experiment right after ESA published SPFC finalists in March 2003. Detailed plans of our experiment had already been done during the competition, see figure 5, so we could start to build the actual experiment immediately. Most of the work was done in Automation Technology Laboratory in HUT and in Protoshop Oy facilities in Otaniemi. Because exact locations of experiment-attaching holes were given by the organizers, every hole had to be drilled exactly right.

Also the camera, laser, sample container and the mirror had to be fixed precisely at calculated places, so that the desired phase angles could be achieved. A big challenge was also to build the experiment so that minimum number of bolts would point outside from the protective cover, and thus minimize the number of potentially harmful sharp edges pointing from the experiment. Welding was not allowed in any part of the supporting structure.

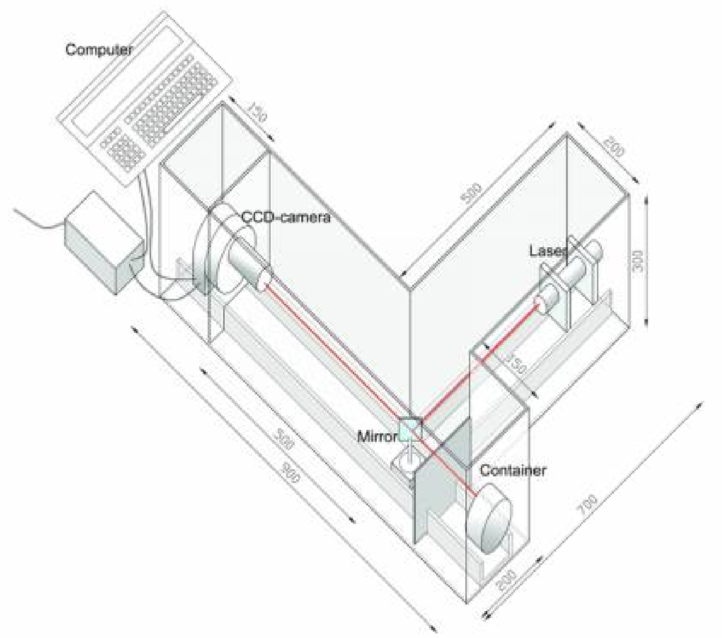

Figure 5: First detailed construction scheme showing experiment dimensions. Note that the mirror is pointing wrong by 90 degrees, i.e. first scheme was not flawless.

The main components of our experiment are presented in figure 5. The CCD-camera shown was a professional level SBIG ST-8E camera, borrowed from the Department of Astronomy at the University of Helsinki. The camera's maximum resolution is 1530 x 1020 pixels and it is specially designed for astronomical purposes. This means that the CCD-chip is flawless, i.e. no software correction for pixels is needed. Due to the camera's high price, about 6000 euros [11], we had to get travel insurance for the camera. For the camera optics, a Nikon Single Lens Reflex (SLR) camera lens was used.

In ground and flight measurements a 1° optical diffuser was installed in front of the optics to avoid laser speckle, i.e. interference maximums caused by the rough reflecting surface. The right intensity is important because the CCD-camera works as a linear detector only between some minimum and maximum integrated intensity, which are affected by the lens aperture size and exposure time. During the Parabolic Flight Campaign (PFC), the aperture of the lens was almost shut and an exposure time of 0.5s was used. The camera was controlled with a laptop through a parallel port connection. Only one exposure could be taken in one microgravity phase, because the readout time of the CCD-camera was about 15 seconds. The SBIG ST-8E camera was found to be very stable in quantum efficiency, i.e. sensitivity to light intensity does not change in time. This was a particularly good feature during the PFC, because we did not need to use parabolas for taking reference frames.

Our laser was also borrowed from FGI. The laser was a Powertechnology Inc. PM-series class 2 diode laser, with a wavelength of 670nm and maximum power of 5mW. We measured the stability of output intensity to be less than 1%, if the laser was turned on only during the measurements, i.e. laser is turned off between parabolas. If the laser is not switched off between the parabolas, then the stability is only about 3%. The instability was mostly due to the battery recharge and discharge effects. The laser was separated to its own circuit so the power supply would disturb the laser's stability as little as possible. This was done using a relay, which connects the laser circuit when all the switches are on.

The beamsplitter and light trap were provided by the Department of Astronomy, and a Spectralon white reference plate by the FGI. The beamsplitter chosen was a Melles-Griot plate with 50/50 reflectance/transmittance ratio. They are calibrated to 45° angle of incidence, which is ideal for the angles used in our experiment. The light trap was needed to catch the light passing through the beamsplitter so that it would not reflect from walls and affect the measurement.

The sample container, sample shaker and the rest of the electronics were made in the Automation Laboratory in HUT. The sample container had to be built with exactly calculated dimensions because we had only a limited amount of olivine basalt we could use. The container also had to be wide enough for the light beam to move through all phase angles, and the depth had to be deep enough to ensure that no reflections from the back wall could occur. The final version of the sample container, shown in figure 6, had outer measurements of 7x3x3cm, and was attached to four springs so it could move in other directions but not towards the camera. The shaker was attached so that when the motor turns, it hits the container once every cycle. The motor was intended to run for two seconds in zero gravity and then be turned off. The springs then slow the movement of the container enough so that the measurement can be taken.

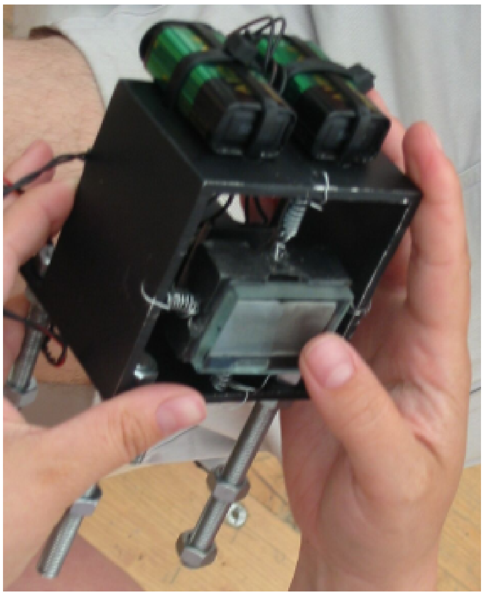

Figure 6: Springs are used to hold and move the sample container.

Our chosen sample material was olivine basalt originating from a lava flow of Pic d'Ysson, France. This is the same kind of basaltic lava that is represented in rocks returned by Apollo astronauts, so the sample could be assumed to be good Lunar maria regolith analog. The sample grain size was chosen to be between 75-250μm, so that Van der Waals forces would not be too significant. The shape of the sample material was examined using a Scanning Electron Microscope (SEM), see figure 16. The SEM images were taken in the Laboratory of Rock Engineering in HUT.

All experiment parts, except the laptop computer, are mounted on a rack made of U-profile aluminum bars and covered with two rectangular aluminum tubes, see figure 7. The tubes have three purposes; they prevent diffuse background light from interfering with the measurements, prevent the laser beam from getting out from the experimental setup, and form a protective casing for the experiment. The laptop is attached to the aluminum bars with L-shaped attachment bars right next to the rest of the experiment setup. The whole experiment had to be designed to withstand a 9g crash load into the direction of the cockpit and slightly smaller forces in other directions. Finally all the edges of the experiment had to be padded to prevent possible injuries to experimenters during microgravity phases, see figure 8.

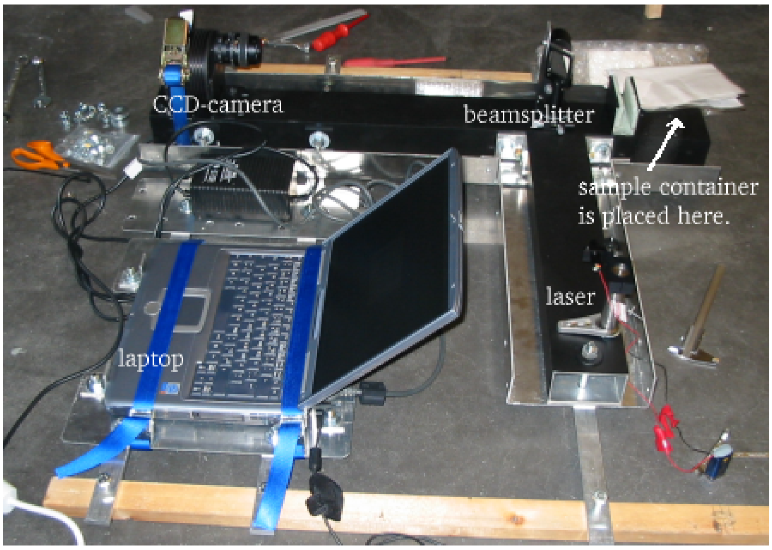

Figure 7: Experiment setup without protective aluminium tubes.

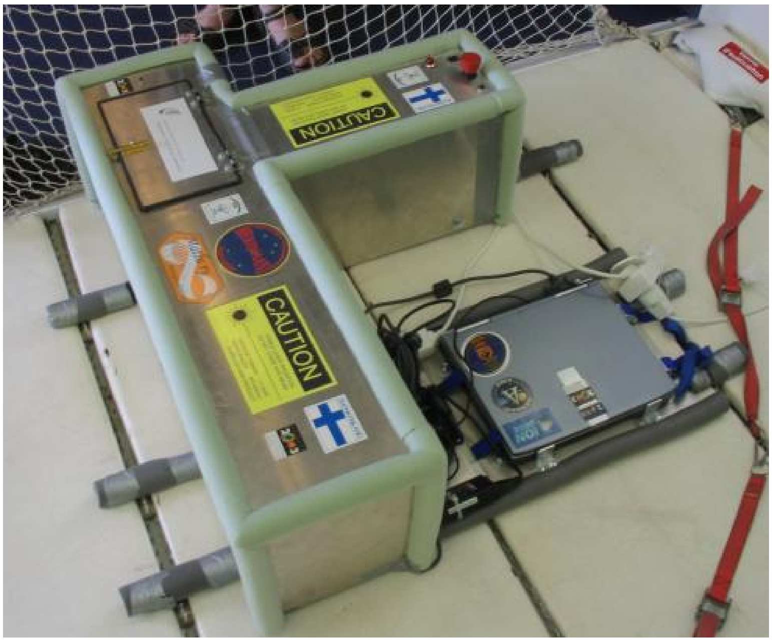

Figure 8: Experiment as fully assembled and installed on the plane.

Security issues made the electrical connections, shown in figure 9, quite complex. A ground fault interrupter was needed for devices connected to 220 V-AC, in our case for the laptop and CCD-camera. It is meant to protect the experiment from electrical shocks by interrupting the circuit when there is a difference between the incoming and outgoing currents. Such a difference means a leakage current from some part of the experiment and could thus produce a dangerous shock hazard. The ground fault interrupter had to be adjusted to a maximum of 30mA difference current. Also a fast fuse was required to be integrated just above the maximum electrical consumption of the experiment, which in our case was 4A. One emergency pushbutton had to be also implemented on the experiment. It had to cut-off both the AC and DC powers.

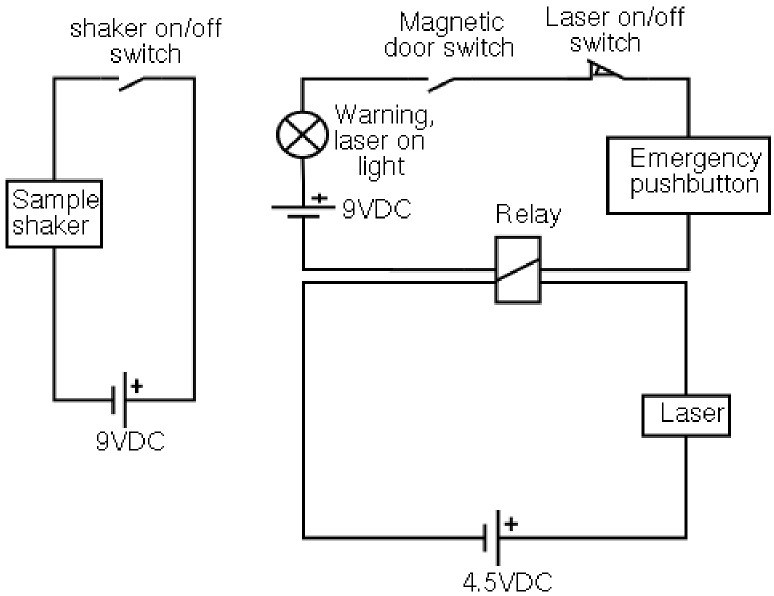

Figure 9: Scheme of electrical DC-connections.

3.2 Measurements

Our experiment flew on two separate flights with two team members on each flight. Jyri Näränen and I flew on the first, and Ville Saarinen and Mikael Granvik on the second. The first flight was completely successful and 31 parabolas were obtained. The second flight was not so successful due to technical and medical difficulties, and only 20 parabolas were obtained. Altogether, the experiment experienced 19 minutes of microgravity.

During the familiarization flight we learned that the sample was very fluid and also reacted significantly to very small forces. Because of that, the first experiment parabola was used to test the shaker motor, and it showed rather clearly that the motor gave too strong impulses to the container.

Thus the container was shaken manually few seconds before each parabola. The springs continued to move the sample after that until the image was taken.

After the flight we were given the gravimeter data taken during the parabolic flights. The stability of microgravity obtained from the data can be seen in figure 10. The gravity is about 100 times smaller than the gravity experienced on the Earth, with the biggest fluctuations experienced in z-direction, i.e. in up-down direction. The fluctuations were much smaller in other directions.

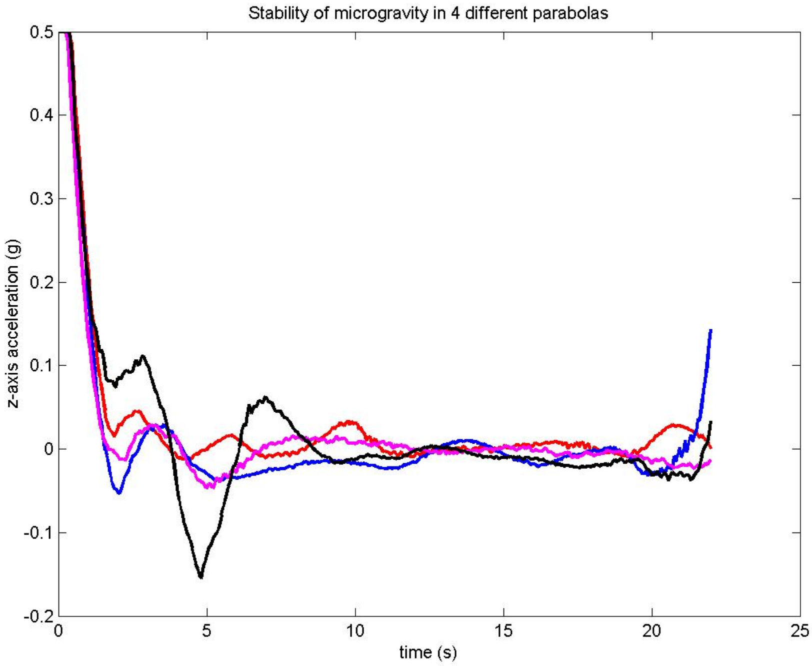

Figure 10: Stability of microgravity in up-down direction.

The CCD-frames were processed by Jyri Näränen with Research Inc. Interactive Data Language (IDL) software using Gaussian fit to obtain the maximum value of the image. The routine also takes into account the ellipticity of the laser spot with different phase angles.

4 Results

The first result gained from our experiment was the observed behavior of the small grain size sample in microgravity. Our target was to make the dust flow as a loose cloud, but in practice, the sample was cohesive and moved liked a liquid from side to side. We had already noticed in the familiarization flight that the sample needed only light movements to be distributed homogenously. If the movement perpendicular to CCD-camera was too violent, the dust just moved from side to side. Gentle movements towards and away from the camera seemed to distribute the dust most efficiently for our purposes. With manual shaking the dust is distributed quite evenly, but the repeatability is unfortunately mostly lost.

From the total of 50 parabolas we obtained 36 usable pictures, which is an acceptable result when operating in such a demanding new environment. Three pictures were taken from each phase angle, with the exception of 6 pictures for the zero phase angle. This means that we obtained 11 data points between $0° - 4°$ phase angles. This flight data is shown in figure 11. The error bars represent standard deviation (1σ).

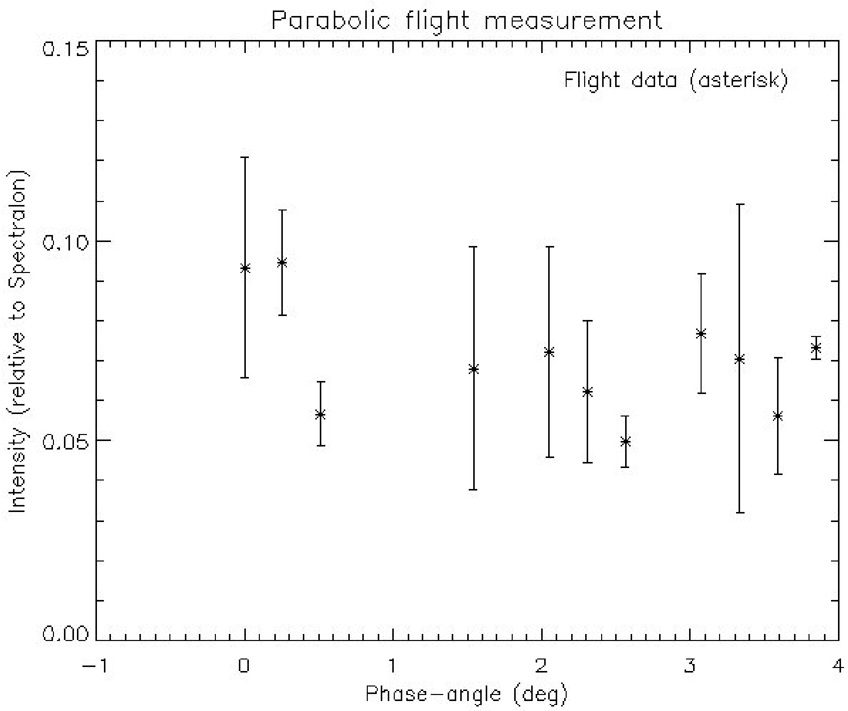

Figure 11: The 11 flight data points obtained.

It is interesting to compare the flight data with other laboratory measurements. The comparison between flight data, 1g dust and sample container is shown in figure 12. The flight data and sample container data show indisputable correlation, but the opposition spike in the flight data indicates that there was also a different signal involved. A quicker detector could have clarified the situation by being able to receive more than one picture per parabola. Also an extra camera inside the experiment would have shown what we were really seeing in each picture. The biggest accomplishment however was the proof that these kinds of experiments can be done in a challenging microgravity environment.

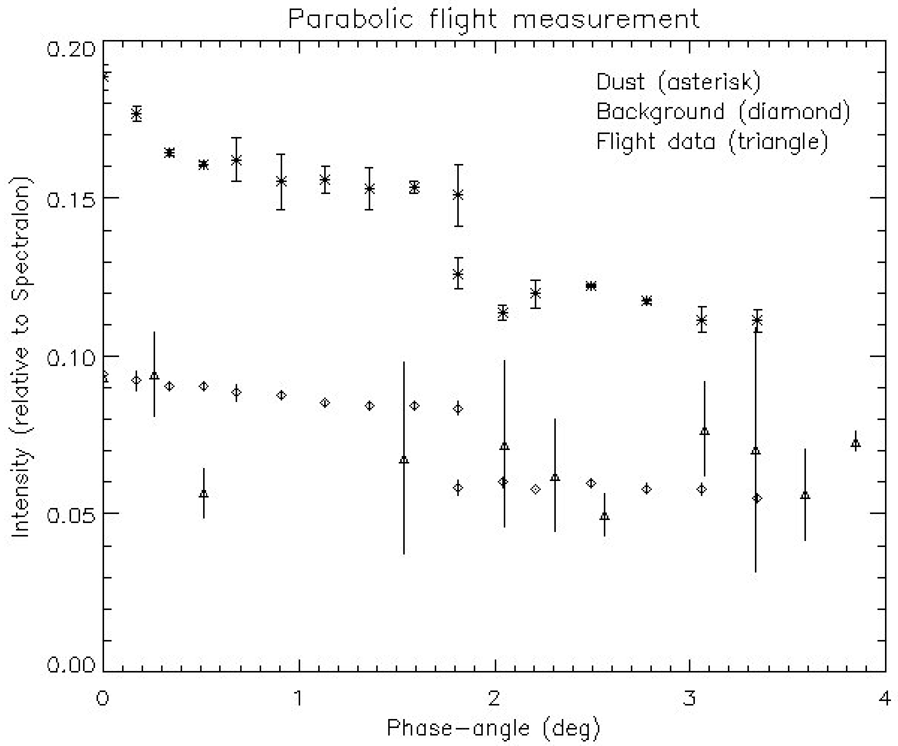

Figure 12: The flight data compared to sample container and dust in Earth's gravity.

4.1 Effect of packing density

Further measurements with the experiment setup were done in the laboratory environment to find the effect of packing density on the light backscattering. These results are shown in figure 13. The results clearly show that an increase in packing density also increases the reflectance. Also the width of the opposition effect is broadened. This is contrary to some previous investigations by Shukaratov et al. [12] and by Capaccioni et al. [13]. This is very likely due to use of different sample materials, therefore indicating the need for more measurements with various other materials.

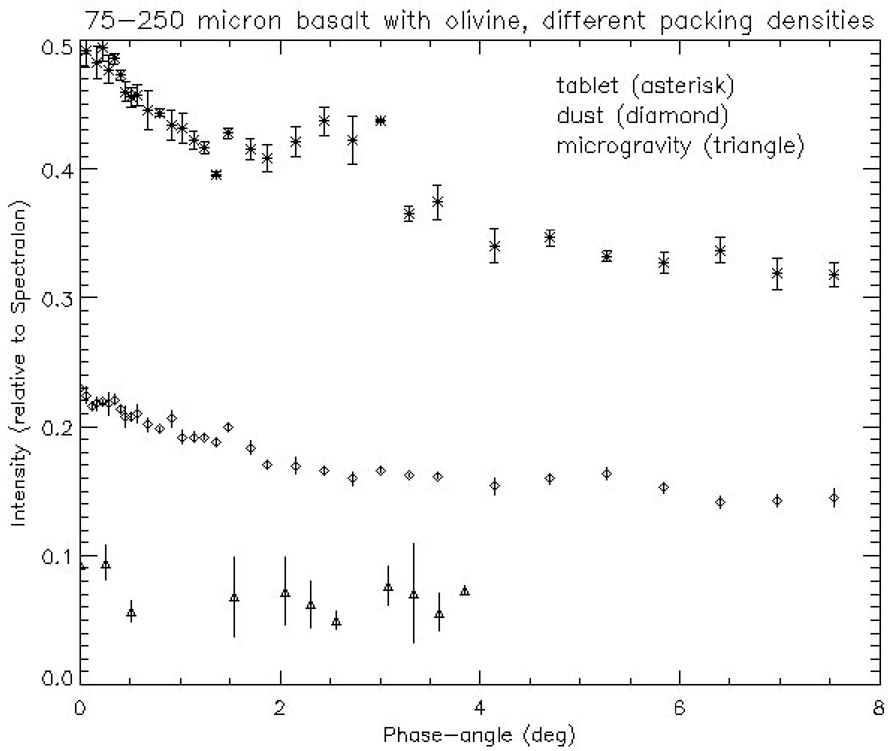

Figure 13: backscattering from olivine basalt with different packing densities; 10g tablet, 1g dust and microgravity dust.

4.2 Results consistency

To get some reference on what we might see and expect from our measurements, the sample container and dust backscattering was also measured in the ground, see figure 14. This measurement also shows that the plain black sample container does not show any opposition effect, as was expected, but the dust instead exhibits an opposition brightening.

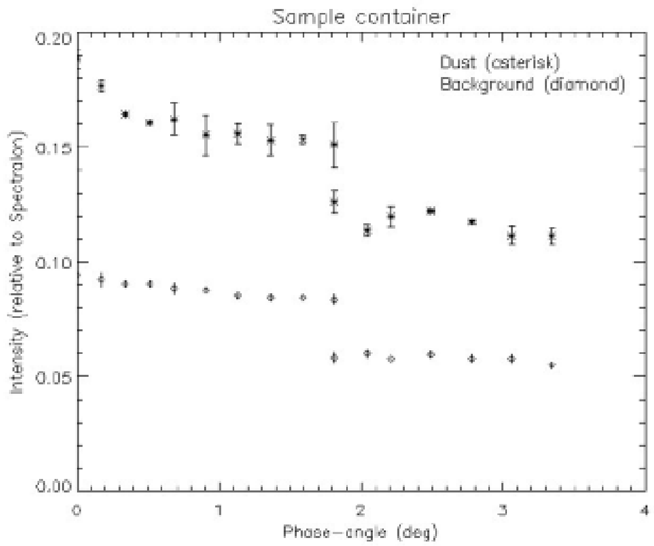

Figure 14: Sample container and dust measured in 1g. The uncontinuity in 1.8 degree phase angle is due to changes in laboratory setup.

The consistency of measurements can be also examined through Spectralon plate reference measurements. Each angle was calibrated using the Spectralon measurements shown in figure 15.

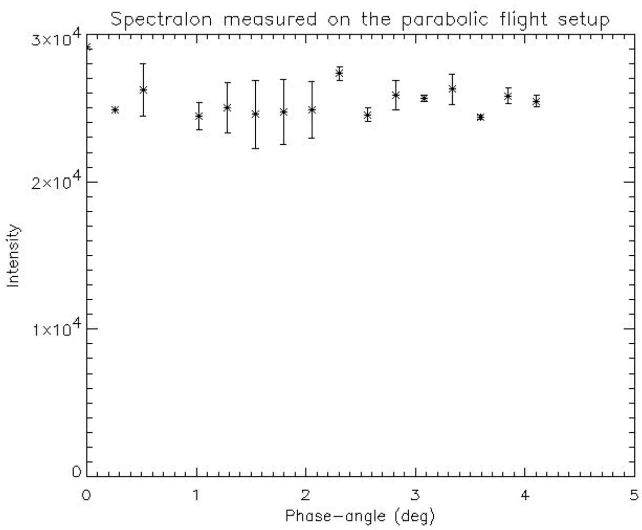

Figure 15: The reference measurements made with Spectralon plate.

4.3 Conclusions

Our measurements showed a strong increase in both reflectance and opposition effect amplitude under compaction. Also a broadening of the opposition effect width was observed. The experiment also showed that it is feasible to conduct light scattering measurements in a microgravity environment. Important experience about shaking the sample using springs and motor was also obtained.

4.4 Future plans

As mentioned before, the sample shape was studied using SEM images. The original purpose was to use the SEM-images to obtain the shape parameters for the measured sample material. This was not very successful because the shape distribution was found to be too complex for available shape recognition routines. Thus developing models to give proper shape parameters could be one reasonable task in the future. More measurements with different materials would also be needed, as mentioned in the previous section.

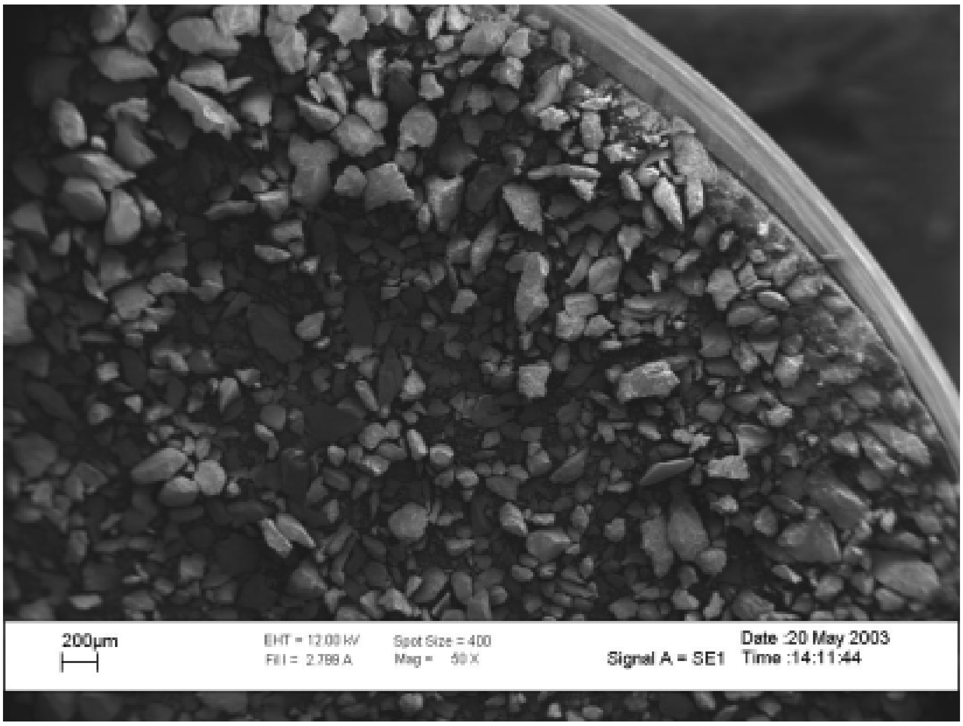

Figure 16: SEM image showing detailed sample structure.

After obtaining enough valid measurements and developing suitable mathematical models for surface parameters, the results could be used in remote sensing to determine physical properties of a regolith over astronomical distances. The small phase angle measurements are closely linked to Bidirectional Reflectance Distribution Function (BRDF) studies with larger phase angles. BRDF studies are very important for remote sensing because BRDF is needed for the correction of the viewing and illumination angle effects, for land cover classification, and multiple other applications. There are also many measurements from atmosphereless, dusty bodies in the Solar system showing the opposition effect [14], which could then be better understood. For example, ESA lunar mission SMART-1 has an advanced imaging system AMIE [15], which produces data in the opposition region. Having laboratory data of scattering in small gravity environments helps us link SMART-1 data to physical parameters, i.e. to Lunar surface properties.

Our work was presented at the Avaruus 2003 exhibition and at least four different newspapers wrote an article about our experiment. Our team's principal investigator, Jyri Näränen, also wrote partly his master's thesis using the experiment results [6]. Jyri and Jyri's Master Thesis were also the main references for this assignment. There are also two publications waiting for acceptance; one article for Astronomy & Astrophysics journal [16] and one paper for the 55th International Astronautical Federation (IAF) congress in Vancouver [17]. There should also be about a twenty minute program in TV1 about the experiment, but it has not yet been scheduled for airing.

Abbreviations

BRDF Bidirectional Reflectance Distribution Function

ESA European Space Agency

FGI Finnish Geodetic Institute.

HUT Helsinki University of Technology

IAF International Astronautical Federation

IAU International Astronomical Union

IDL Interactive Data Language

PFC Parabolic Flight Campaign

SEM Scanning Electron Microscope

SLR Single Lens Reflex

SPFC Student Parabolic Flight Campaign

References

[1] Worms, Jean-Claude et al., 1999, Results of the PROGRA2 Experiment: An Experimental Study in Microgravity of Scattered Polarized Light by Dust Particles with Large Size Parameter, Icarus 142, p.281

[2] Finnish students on a parabolic flight campaign in 2002. http://www.esa.int/export/esaCP/ESAYOOZPD4D_Finland_0.html

[3] Novespace English homepage. http://www.novespace.fr/VEnglish/welcome_a.html

[4] ESA parabolic flight campaigns, introduction. http://www.estec.esa.int/spaceflight/parabolic/intropar.htm

[5] Peltoniemi J.I. and Lumme K. 1992 Light scattering by closely packed particulate media, Journal of the Optical Society of America

[6] Jyri Näränen, University of Helsinki, Astronomy Master's thesis 2003. Light scattering measurements of planetary regolith analogs at small phase angles.

[7] Bruce Hapke, The History of the Fairy Castles http://www.hq.nasa.gov/office/pao/History/alsj/Fcastles.htm

[8] Opposition Effect and shadow hiding. http://www.sundog.clara.co.uk/atoptics/oppos1.htm

[9] B. W. Hapke, J. L. Piatek (U. of Pittsburgh), R. M. Nelson, W. D. Smythe, A. S. Hale (JPL) Coherent Backscatter Opposition Effect from Scratches on Solid Surfaces http://www.aas.org/publications/baas/v35n4/dps2003/350.htm

[10] Kaasalainen, Sanna, 2002, Backscattering of Light From Solar System Ices and Regoliths, Academic Dissertation, Observatory, University of Helsinki

[11] SBIG ST-8E camera specifications http://www.sbig.com/sbwhtmls/st8.htm

[12] Shkuratov YU., Ovcharenko A., Zubko E., Miloslavskaya O., Muinonen K., Piironen J., Nelson R., Smythe W., Rosenbush V. and Helfstein P 2002 The opposition effect and negative polarization of structural analogs for planetary regoliths, Icarus.

[13] Capaccioni F., Cerroni P., Barucci M. A., and Fulchignoni M. 1989 Phase curves of meteorites and terrestrial rocks: Laboratory measurements and applications to asteroids, Icarus.

[14] Piironen, Jukka, 1998, Photometry of Asteroids at Small Phase Angles with Related Laboratory Measurements, Academic Dissertation, Observatory, University of Helsinki

[15] Muinonen, Karri et al., 2002, The SMART-1 AMIE Experiment: Implications to the Lunar Opposition Effect, Planetary and Space Science 50, p.1339

[16] Astronomy & Astrophysics Journal Homepage, http://www.edpsciences.org/aa/

[17] International Astronautical Congress 2004 homepage, http://www.iac2004.ca/